



Soft Computing in the Design and Manufacturing of Composite Materials

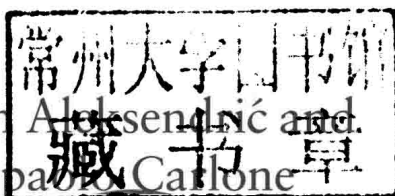
Applications in brake friction and
thermoset matrix composites

Dragan Aleksendrić
Pierpaolo Carlone

Soft Computing in Design and Manufacturing of Composite Material

*Applications in brake friction and
thermoset matrix composites*

Dragan Aleksenđrić and
Pierpaolo Carlone



AMSTERDAM • BOSTON • CAMBRIDGE • HEIDELBERG • LONDON
NEW YORK • OXFORD • PARIS • SAN DIEGO
SAN FRANCISCO • SINGAPORE • SYDNEY • TOKYO

Woodhead Publishing is an imprint of Elsevier



Woodhead Publishing is an imprint of Elsevier
80 High Street, Sawston, Cambridge, CB22 3HJ, UK
225 Wyman Street, Waltham, MA 02451, USA
Langford Lane, Kidlington, OX5 1GB, UK

Copyright © D Aleksendrić and P Carlone, 2015

No part of this publication may be reproduced, stored in a retrieval system or transmitted in any form or by any means electronic, mechanical, photocopying, recording or otherwise without the prior written permission of the publisher. Permissions may be sought directly from Elsevier's Science & Technology Rights Department in Oxford, UK: phone (+44) (0) 1865 843830; fax (+44) (0) 1865 853333; email: permissions@elsevier.com. Alternatively you can submit your request online by visiting the Elsevier website at <http://elsevier.com/locate/permissions>, and selecting Obtaining permission to use Elsevier material.

Notice

No responsibility is assumed by the publisher for any injury and/or damage to persons or property as a matter of products liability, negligence or otherwise, or from any use or operation of any methods, products, instructions or ideas contained in the material herein. Because of rapid advances in the medical sciences, in particular, independent verification of diagnoses and drug dosages should be made.

British Library Cataloguing-in-Publication Data

A catalogue record for this book is available from the British Library

Library of Congress Control Number: 2014948681

ISBN 978-1-78242-179-5 (print)

ISBN 978-1-78242-180-1 (online)

For information on all Woodhead Publishing publications
visit our website at <http://store.elsevier.com/>

Typeset by RefineCatch Limited, Bungay, Suffolk



**Working together
to grow libraries in
developing countries**

www.elsevier.com • www.bookaid.org

Printed in the United States of America

Soft Computing in Design and Manufacturing of Composite Material

Related titles:

Failure mechanisms in polymer matrix composites
(ISBN 978 1 84569 750 1)

Materials, design and manufacturing for lightweight vehicles
(ISBN 978 1 84569 463 0)

Introduction to aerospace materials
(ISBN 978 1 85573 946 8)

List of figures

2.1	The process of product development	10
2.2	Top-down–bottom-up approach to the development of a braking system regarding the properties of a friction pair	11
3.1	Temperature and degree-of-cure profiles for a Shell Epon 9420/9470/537 resin	18
3.2	Temperature and viscosity profiles for a Shell Epon 9420/9470/537 resin	19
3.3	Energy intensity of composite-manufacturing processes	24
3.4	Schematic view of the pultrusion process	24
3.5	Synergetic effects of formulation and manufacturing conditions on friction and wear of a brake friction material	30
3.6	A flash mould method for brake friction material manufacturing	32
3.7	Flash mould method – a mould cavity	33
3.8	Positive moulding – compression process without a breathing cycle	34
4.1	The basic architecture of an artificial neural network	40
4.2	The learning process of an artificial neural network	41
4.3	The process of development of an artificial neural network model	43
4.4	Typical structure of a layer-recurrent neural network	44
4.5	Dynamic neural model of disc brake operation based on a layer-recurrent network	44
4.6	Geometric interpretation of the finite difference approximation of the first derivative	49
4.7	Element type and dimensionality	51

4.8	Mesh and dual mesh in vertex-centred FVM (a, b) and cell-centred FVM (c, d). Control volumes are defined by the grey-coloured areas	52
4.9	The basic cycle of a genetic algorithm	54
4.10	A hybrid ANN–GA optimization model	56
5.1	Modelling issues and reciprocal interactions in composite-manufacturing processes	65
5.2	Time–temperature–transformation diagram for a generic thermoset resin	69
5.3	Micro-, meso- and macro-scales in composite-manufacturing simulation	75
5.4	Graphical scheme of the evaluation of the Morishita index	76
5.5	Graphical scheme of the evaluation of the Ripley function, showing the definition of $I_k(r)$ and the weight factor: (a) $w_k = 1$, (b) $w_k \neq 1$	77
5.6	L function: comparison with the Poisson distribution	78
5.7	Lay-up of a process and corresponding finite element three-dimensional scheme	80
5.8	Lay-up of the process and corresponding finite element one-dimensional scheme	82
5.9	Temperature profiles: numerical results and reference data	84
5.10	Degree-of-cure profiles: numerical results and reference data	84
5.11	Viscosity profiles: numerical results and reference data	85
5.12	Viscosity profiles, showing the process window	86
5.13	Flow chart of the generation algorithm for the random RVEs	88
5.14	RVE perturbation: (a) 50, (b) 500, (c) 1000, (d) 5000 iterations	89
5.15	Statistical analysis of the RVEs: (a) Ripley L function; (b) pair distribution function; (c) histogram of radius distribution; (d) Morishita number	90
5.16	Micro-scale computational domain and boundary conditions	91

5.17	Thermal flux along the transverse direction	92
5.18	Temperature and degree of cure at centre	94
5.19	Multi-physics involved in the pultrusion process and related interactions	95
5.20	Centreline pressure rise in the tapered region of the die	98
5.21	Streamlines of resin flow in the tapered region of the die	99
5.22	(a) Case study, and discretization of the cross-section: (b) FDM and (c) FEM	103
5.23	Temperature profiles in the pultrusion die	105
5.24	Cure profiles in the pultrusion die and comparison with reference data	106
5.25	Schematic view of the pultrusion domain for the composite rod. All dimensions are in millimetres	109
5.26	Temperature and degree of cure profiles: comparison of the outcomes of the present calculations with the reference data	110
5.27	Temperature and degree of cure profiles: comparison of the outcomes of the present calculations with the reference data	111
5.28	Pulling force and phase changes	112
5.29	Viscosity profiles and virtual workpiece radius	113
5.30	Flow front after (a) 10 s, (b) 30 s, (c) 60 s, (d) 120 s, (e) 180 s and (f) 300 s since the beginning of impregnation	117
5.31	Resin flow front: numerical and analytical results	117
5.32	(a) Solid model and (b) meshed computational domain	118
5.33	Resin front after (a) 15 s, (b) 3 min, (c) 6 min, (d) 9 min, (e) 18 min and (f) 30 min	119
5.34	Computational domain and boundary conditions: (a) calculation of transverse permeability; (b) calculation of longitudinal (axial) permeability	120
5.35	Transverse-permeability results	121
5.36	Axial-permeability results	122

5.37	Flow front, and temperature and degree of cure distributions at different time instants for $T_{\text{ext}} = 25^\circ\text{C}$	125
5.38	Flow front, and temperature and degree of cure distributions at different time instants for $T_{\text{ext}} = 50^\circ\text{C}$	126
5.39	Flow front, and temperature and degree of cure distributions at different time instants for $T_{\text{ext}} = 100^\circ\text{C}$	127
5.40	Viscosity distributions at $t = 300$ s for $T_{\text{ext}} =$ (a) 25°C , (b) 50°C and (c) 100°C	127
5.41	Numerical and analytically computed (using the mean viscosity value) resin flow fronts	128
5.42	(a) Experimental set-up and (b) results from dielectric monitoring of flow through a dual-scale porous medium	130
5.43	Mass balance in an elementary control volume including saturation effects	131
5.44	Tow saturation scheme	131
5.45	Numerical and analytically computed (using the mean viscosity value) resin flow fronts	132
5.46	(a) Pultrusion process and (b) section considered for optimization	140
5.47	Temperature profiles in the pultrusion die in the reference case	141
5.48	Cure profiles and degree of cure distribution in the final cross-section of the workpiece in the reference case	141
5.49	Convergence plots using different selection criteria: (a) uniform, (b) roulette and (c) tournament	144
5.50	Control temperatures of the die heating zones, according to (a) the genetic optimization routine and (b) the hybrid routine	147
5.51	Temperature and cure profiles and distribution of the degree of cure in the final cross-section of the workpiece, after the genetic optimization routine using the FEM	148
5.52	Temperature and cure profiles and distribution of the degree of cure in the final cross-section of the workpiece, after the hybrid optimization routine using the FEM	148

5.53	Temperature and cure profiles and distribution of the degree of cure in the final cross-section of the workpiece after the genetic optimization routine (test case Tc4, using the FEM)	151
5.54	Temperature and cure profiles and distribution of the degree of cure in the final cross-section of the workpiece after the hybrid genetic routine (test case Tc4)	153
5.55	Representation of a four-step thermal cycle, including the final cooling	156
5.56	Optimal thermal cycle and temperature and degree of cure profiles as suggested by the simulated annealing algorithm ($\lambda_k = \lambda_2$)	159
5.57	Optimal thermal cycle and temperature and degree of cure profiles as suggested by the modified simulated annealing algorithm ($\lambda_k = \lambda_1$)	160
5.58	Performance of simulated annealing algorithm: (a) fitness scores at the end of the optimization and (b) computational times	161
5.59	Substitution	163
5.60	Swapping	164
5.61	Optimal thermal cycle and temperature and degree of cure profiles as suggested by the algorithm GA1 ($\lambda_k = \lambda_2$)	164
5.62	Optimal thermal cycle and temperature and degree of cure profiles as suggested by the algorithm GA2 ($\lambda_k = \lambda_2$)	165
5.63	Performance of genetic algorithms: (a) fitness scores at the end of the optimization and (b) computational times	167
5.64	Artificial neural network model for prediction of the behaviour of friction materials	172
5.65	Cold performance predictions using Bayesian regulation algorithm	181
5.66	Cold performance predictions using resilient backpropagation algorithm	183
5.67	Cold performance predictions using Levenberg–Marquardt algorithm	184

5.68	Cold performance predictions using scaled conjugate gradient algorithm	185
5.69	Cold performance predictions by gradient descent algorithm	186
5.70	Cold performance 1 – Comparison between real and predicted results versus initial speed for $p = 40$ bar	189
5.71	Cold performance 1 – Comparison between real and predicted results versus initial speed for $p = 60$ bar	189
5.72	Cold performance 1 – Comparison between real and predicted results versus initial speed for $p = 80$ bar	190
5.73	Cold performance 1 – Comparison between real and predicted results versus initial speed for $p = 100$ bar	190
5.74	Cold performance 1 – Comparison between real and predicted results versus brake actuation pressure for $v = 80$ km/h	191
5.75	Cold performance 1 – Comparison between real and predicted results versus brake actuation pressure for $v = 100$ km/h	191
5.76	Cold performance 2 – Comparison between real and predicted results versus initial speed for $p = 40$ bar	192
5.77	Cold performance 2 – Comparison between real and predicted results versus initial speed for $p = 60$ bar	194
5.78	Cold performance 2 – Comparison between real and predicted results versus initial speed for $p = 80$ bar	195
5.79	Cold performance 2 – Comparison between real and predicted results versus initial speed for $p = 100$ bar	195
5.80	Cold performance 2 – Comparison between real and predicted results versus brake actuation pressure for $v = 80$ km/h	196
5.81	Cold performance 2 – Comparison between real and predicted results versus brake actuation pressure for $v = 100$ km/h	196
5.82	Fading performance of friction material F_{T1}	208
5.83	Prediction of fading performance of material F_{T1} by Bayesian regulation algorithm	209
5.84	Prediction of fading performance of material F_{T1} – real and predicted by Bayesian regulation algorithm	212

5.85	Prediction of fading performance of material F_{T1} by resilient backpropagation algorithm	213
5.86	Prediction of fading performance of material F_{T2} – real and predicted by Bayesian regulation algorithm	214
5.87	Prediction of fading performance of material F_{T1} – real and predicted by neural model BR 26_8_4_2_1 (training data set F1–F8)	215
5.88	Prediction of fading performance of material F_{T1} – real and predicted by neural model BR 26_8_4_1 (training data set F1–F8)	217
5.89	Prediction of fading performance of material F_{T1} – real and predicted by neural model BR 26_10_5_1 (training data set F1–F8)	218
5.90	Prediction of fading performance of material F_{T2} – real and predicted by neural model BR 26_10_5_1 (training data set F1–F8)	220
5.91	Examples of changes in measured parameters during a braking cycle: (a) braking torque, (b) speed, (c) application pressure and (d) brake interface temperature	226
5.92	Neural modelling of the wear of friction materials	228
5.93	Number and positions of wear-measuring points	228
5.94	Comparison between real and predicted specific wear rates (friction materials F_{T1} , F_{T2} and F_{T3})	234
5.95	Comparison between real and predicted wear volumes of friction material F_{T1} in wear test 1	234
5.96	Comparison between real and predicted wear volumes of friction material F_{T1} in wear test 2	236
5.97	Comparison between real and predicted wear volumes of friction material F_{T1} in wear test 3	236
5.98	Comparison between real and predicted wear volumes of friction material F_{T2} in wear tests 1, 2 and 3	237
5.99	Comparison between real and predicted wear volumes of friction material F_{T3} in wear tests 1, 2 and 3	239
5.100	Predicted specific wear rate versus influence of the manufacturing and operation conditions of the friction material	240

5.101	Predicted specific wear rate versus influence of the formulation, manufacturing and operation conditions of the friction material	240
5.102	Single-ended full-scale inertia dynamometer	245
5.103	Schematic illustration of the artificial neural network model for wear	248
5.104	Schematic illustration of the neural model used for optimization of manufacturing parameters	249
5.105	Illustration of the hybrid neuro-genetic optimization model used for optimization of manufacturing parameters	250
5.106	Optimization of the manufacturing parameters of brake friction material F_{T1} for a brake interface temperature of 100°C	251
5.107	Optimization of the manufacturing parameters of brake friction material F_{T1} for a brake interface temperature of 175°C	253
5.108	Optimization of the manufacturing parameters of brake friction material F_{T2} for a brake interface temperature of 100°C	255
5.109	Optimization of the manufacturing parameters of brake friction material F_{T2} for a brake interface temperature of 175°C	256
5.110	Optimization of the manufacturing parameters of brake friction material F_{T3} for a brake interface temperature of 100°C	258
5.111	Optimization of the manufacturing parameters of brake friction material F_{T3} for a brake interface temperature of 175°C	260
5.112	Optimal values of manufacturing parameters of brake friction materials F_{T1} , F_{T2} and F_{T3} for a brake interface temperature of 100°C	260
5.113	Optimal values of manufacturing parameters of brake friction materials F_{T1} , F_{T2} and F_{T3} for a brake interface temperature of 175°C	261
5.114	Synergistic effect of pressure and speed on the brake factor C (cold brake)	265

5.115	Changes in brake factor C versus synergistic pressure–speed influence	266
5.116	Changes in braking torque during a braking cycle (low brake actuation pressure)	268
5.117	Optimization of brake actuation pressure versus braking torque (pedal travel 40%)	269
5.118	Optimization of brake actuation pressure versus braking torque (pedal travel 62%)	271

List of tables

5.1	Physical properties and concentrations of materials	82
5.2	Parameters of resin kinetics	83
5.3	Parameters of the rheological model	84
5.4	Physical properties and concentrations of materials	92
5.5	Normalized conductivity	93
5.6	Parameters of resin kinetics	94
5.7	Parameters of the rheological model	97
5.8	Temperatures of the six heating platens (°C)	103
5.9	Physical properties of materials	104
5.10	Physical properties and concentrations of materials	109
5.11	Properties of the resin systems	116
5.12	Physical properties and concentrations of the resin	124
5.13	Parameters of the kinetic model	124
5.14	Parameters of the rheological model	125
5.15	Simulation parameters for the flow through a dual-scale preform	132
5.16	Numerical results for the reference case of the considered pultrusion process	142
5.17	Results of genetic algorithm using different selection methods	143
5.18	Influence of the crossover method on the results of the genetic algorithm (roulette selection)	145
5.19	Influence of the mutation rate on the results of the genetic algorithm (roulette selection and uniform crossover)	145
5.20	Numerical results for the reference case of the pultrusion process	146
5.21	Processing parameters for the optimized test cases	149

5.22 Heating-platen temperatures and results provided by genetic optimization using the FDM	150
5.23 Heating-platen temperatures and results provided by hybrid optimization using the FDM	151
5.24 Heating-platen temperatures and results provided by genetic optimization using the FEM	153
5.25 Heating-platen temperatures and results provided by hybrid optimization using the FEM	153
5.26 Cold performance – testing methodology	173
5.27 Friction materials A, B, C, D and E – ranges of proportions of ingredients used (vol%)	175
5.28 Manufacturing parameters	175
5.29 Fraction of the test data set (%) in the error intervals	187
5.30 Speed sensitivity – comparison between maximum and minimum values (real and predicted) (cold performance 1, $v_{\text{Initial}} = 20\text{--}100\text{ km/h}$)	188
5.31 Pressure sensitivity – comparison between maximum and minimum values (real and predicted) (cold performance 1, $p = 20\text{--}100\text{ bar}$)	188
5.32 Speed sensitivity 2 – comparison between maximum and minimum values (real and predicted) (cold performance 2, $v_{\text{Initial}} = 20\text{--}100\text{ km/h}$)	193
5.33 Pressure sensitivity 2 – comparison between maximum and minimum values (real and predicted) (cold performance 2, $p = 20\text{--}100\text{ bar}$)	194
5.34 Fading performance – testing methodology	202
5.35 Friction materials F1–F8; F_{T1} and F_{T2} – ranges of proportions of ingredients used (vol%)	203
5.36 Ranges of manufacturing parameters	204
5.37 Changes in brake factor C versus temperature – comparison between real and predicted values	211
5.38 Comparison of the prediction capabilities of neural models	216
5.39 Comparison of the prediction capabilities of neural model BR 26_10_5_1 versus real data	219
5.40 Wear-testing methodology	223